Natural Hazards (2022) 114:367–387
https://doi.org/10.1007/s11069-022-05393-w

ORIGINAL PAPER

A long-term analysis of thundersnow events over the Marmara Region, Turkey

Veli Yavuz[1,2] · **Anthony R. Lupo**[2] · **Neil I. Fox**[2] · **Ali Deniz**[1,3]

Received: 18 February 2022 / Accepted: 28 April 2022 / Published online: 23 May 2022

Abstract

This study aimed to reveal the temporal statistics, formation mechanisms, suitable land/sea surface (LS/SS) and upper-level atmospheric conditions, and predictability of thundersnow (TSSN) events that occurred between 2000 and 2021 in the Marmara Region with atmospheric stability indexes. Aviation reports from 11 airports were analyzed throughout the period, and no TSSN events were found at four airports. A total of 19 TSSN events were identified, and six events were found in 2015, when the sea-effect snow (SES) mechanisms were observed four times. The majority of TSSN events were of very short duration (0–1 h), and no significant trend was observed in terms of intraday distribution. SES mechanism was observed in 17 of the 19 TSSN events, and the dominance of northern flows was detected at all airports and at the sub-inversion upstream levels. In terms of air-sea interaction, suitable temperature differences between the SS and 850/700 hPa (17 °C and 27 °C on average), and the transfer of heat-moisture fluxes from the SS to the upper-atmosphere were possible in almost all TSSN events. In this way, meteorological parameters were sufficient for the formation and strengthening of the convective layer. In addition, the presence of directional wind shear and the observation of inversion layers restricting convective movements at higher levels instead of near the surface ensured that the moisture requirement, lifting mechanism, and unstable atmospheric conditions required for the formation of TS were provided. The CAPE values were very low for winter TSs. Total Total Index and TQ Index produced the most appropriate results for TSSN prediction.

Keywords Thundersnow · Sea-effect snow · Snow bands · TSSN · Stability index · Marmara region

✉ Veli Yavuz
yavuzv@itu.edu.tr; veliyavuz@missouri.edu

1 Faculty of Aeronautics and Astronautics, Department of Meteorological Engineering, Istanbul Technical University, ITU Maslak Campus, 34469 Maslak, Istanbul, Turkey

2 Atmospheric Science Program, University of Missouri, 302 E ABNR, Columbia, MO 65211, USA

3 Eurasia Institute of Earth Sciences, Istanbul Technical University, ITU Maslak Campus, 34469 Maslak, Istanbul, Turkey

1 Introduction

A thunderstorm (TS) is a weather phenomenon commonly characterized by lightning and thunder, causing heavy rainfall, strong winds (also wind gusts) and may also generate tornadoes (Yavuz et al. 2020). The relatively high moisture content of the air parcel, the presence of buoyancy forces that will carry the air parcel upwards (i.e., convection, convergence, orographic ascent, or frontal lifting) and the unstable atmospheric conditions are important in terms of the formation of the necessary atmospheric environment for the occurrence of TS (Ackerman and Knox 2002; Özdemir et al. 2017; Wahiduzzaman et al. 2022). In addition, vertical wind shear is often critical in the formation of TS (Doswell and Evans 2003; Özdemir 2021; Yavuz et al. 2022a). TSs can occur mostly with heavy rain (TSRA) (Özdemir et al. 2019), occasionally singularly (TS), and rarely with snow (TSSN) (Crowe et al. 2006; Bech et al. 2013) and sleet (TSSNRA) (Bech et al. 2013).

TSSN, also known as a convective snowfall event, usually occurs with synoptic-scale systems, and sometimes occurs at meso-scale depending on local effects (i.e., coastal convergence-frictional convergence, orographic ascent). Schultz and Varek (2009) described it as a rare/unusual weather phenomenon when compared with other snowfall and thunder events. The fact that lightning and thunder events occur mostly during seasonal transitions and spring months when the atmospheric instability is high, and that TSSN occurs in the winter season when more stable atmospheric conditions prevail, strengthens the definition of "rare weather phenomenon." TSSN has the potential to significantly reduce horizontal and vertical visibility with the combination of lightning and snow. This negatively affects land, sea, and especially air transport activities (Wilkinson et al. 2013; Zook 2014). In this study, the TSSN event, which was detected at different times on 12 January 2015 at seven airports in the Marmara Region, led to cancellation of most of the flights due to the severe storm and decrease in visibility because of heavy snowfall (Dunya 2015). This unexpected event also caused people to be more exposed to the possibility of lightning strikes in open areas (for example, skiing activities) (Cherington 2001). Climatological analyses and case studies were carried out mostly for North America and Canada regarding TSSN events (Crowe et al. 2006; Market et al. 2006, 2007). For Europe, Munzar and Franc (2003) examined winter thunderstorms, but did not directly address the thundersnow event.

Curran and Pearson (1971), in their study in which they analyzed hourly surface observations for the United States (USA) between 1968 and 1971, detected TSSN in only 76 reports out of 114,924 reports. Elkins (1987) detected 43 thundersnow events by following the Daily Weather Map series between 1971 and 1986 in the USA. In this study, the origins of cyclones and the air parcel within the cyclone were investigated. Colman's work (1990a, b) classified elevated TS events according to precipitation types (i.e., rain, snow, sleet, etc.), and revealed their meso- and synoptic-scale environmental conditions. Schultz (1999), based on the surface meteorological station data, analyzed the thunders that occurred between October and May for the USA, and found snow in only 1.3% of them.

In studies on convective precipitation in the cold-season, it was stated that atmospheric contents (such as, atmospheric instability, a lifting mechanism and high moisture content) similar to those in the warm-season are required. However, the physical and dynamic processes that produce these contents must be different in the cold-season. Although the TSSN event seems to be a meso-scale event, the effects of synoptic-scale systems were mostly observed in its formation mechanisms (Market et al. 2002). Schultz and Vavrek (2009) revealed a recipe for TSSNs that occur in the USA. Four basic components (moisture, lifting, unstable temperature profile, and cold air) required for TSSN have been determined. It was determined that the moisture source can be met by local sources, as well as by long-distance transport (from Gulf of Mexico), and even in the Great Lakes region, TSSNs were formed by the lake-effect mechanism. Regarding the lifting mechanism, the rising of warm air parcel required for convective storm occurred by frontal systems or orographic effects. Unstable temperature gradient profiles can also occur under the influence of synoptic-scale systems and irregular distributions of upper-level jet streams. Finally, the cold air pool (which must be below the freezing point) was expected to form within the clouds near the ground.

Compared to summer convective TSs, lower convective available potential energy (CAPE) values were observed in winter TSSNs (Stuart 2001; Halcomb and Market 2003; Mäkelä et al. 2013, Kumjian and Dierling 2015). Market et al. (2002) found no direct effect on the time of day occurrence of TSSNs. In the sounding analyses of TSSN events, it was determined that the temperatures were formed below 0 °C in almost all of the atmospheric column from the surface (Çurran and Pearson 1971; Market et al. 2006; Market et al. 2007). In these cases, when the data obtained from the surrounding stations were examined, the effect of cold air advection observed especially in the lower levels of the atmosphere (below relatively warmer and humid air mass) was seen. In the presence of TSSN, although the temperatures in that station decreased to 0 °C and below, 10 °C values were observed in the surrounding stations (Kumjian and Dierling 2015).

The formation types of TSSNs were classified under six sub-classes by Market et al. (2002). These are cyclone, orographic ascent, coastal cyclone, frontal, lake-effect, and upslope. In order for TSSNs to be included in the cyclone class, they must have at least two closed isobars in the contour range of 4 hPa at the start of the event. Such events usually occur near the front (especially the warm front). Two criteria have been set for the orographic class. These should not occur heavily in the surrounding stations and should be substantially different in terms of the characteristics of the surrounding stations. If these events, which occur in isolation from neighboring stations, are observed at more than one station, they may have occurred in this cyclone class. If TSSN is observed at more than one station along the coast in the presence of an open cyclone in the open sea, it is included in the coastal cyclone class. The frontal class includes events occurring at the ends of the region that are typically stable and do not have a well-defined cyclonic circulation. In the events in the lake-effect class, the presence of lake-effect bands is sought, and TSSNs associated or not associated with synoptic-scale systems are found in this class. In upslope events, a weak cyclonic circulation is required in the presence of an anticyclone or a reverse trough (Market et al. 2002).

In this study, the Meteorological Aerodrome Report (METAR) and the Special Aerodrome Reports (SPECI) reports from 11 airports in the Marmara Region were analyzed for a 22-year period between 2000 and 2021. In total, TSSN (thundersnow) was detected in 31 reports and TSSNRA (thundersnow with rain) in four reports. International airports publish half-hourly reports, while national and military airports publish hourly reports. For this reason, a daily scale was preferred to statistical analysis of the TSSN events. Accordingly, 19 TSSN events were identified. Statistical analyses were carried out for TSSN events on a daily, monthly and annual basis, and the atmospheric conditions in which each event occurred were examined in detail. TSSN events were classified according to the formation types, but this classification was slightly different from Market et al. (2002), so that the formation mechanisms of TSSNs occurring throughout the region were more inclusive. Together with these, the changes of meteorological parameters on the land surface (LS), sea surface (SS) and upper atmosphere were analyzed at the meso-scale, and the thermodynamic structure of the events and the atmospheric instability conditions were determined by using the sounding data.

2 Data and methodology

The TSSN events that occurred in the Marmara Region, one of Turkey's seven geographical regions, were analyzed within the period between 2000 and 2021. The region is located around the Marmara Sea, which is an inland sea, and the Black Sea is located to the north. The prevailing wind direction is southwest in summer and northeast in winter. Summers are warm/hot and dry, and winters are mostly rainy. In terms of climate type, it is stated that there is a Mediterranean climate in summer and Black Sea climate types are observed in winter. (Yavuz et al. 2021a). One of Turkey's most important ski resorts is located in the province of Bursa, located in the south of the Marmara Sea. Similarly, Kocaeli Province, located in the north of the Marmara Region, is home to the Kartepe ski resort. There are 11 airports in total within the boundaries of the region. Six of these airports are in the international category, while the rest are in the national and military category (GDSAA 2021). TSSN events and current surface meteorological parameter values were determined and analyzed by examining the METAR and SPECI reports published by the airports throughout the period. While these reports are prepared at half-hourly intervals at international airports in accordance with regional agreements, reports are mostly published at hourly intervals at national airports. One airport examined in the study started to serve in 2011. Although other airports published reports within the period, especially national and military airports do not publish reports in a specific order. In some airports, reports are prepared only during a certain period of the day (for example, in an 8-h period of the day), while at the airports where flights are made regularly at certain hours, reports are published only at those hour intervals. For this reason, the existence of any TSSN events, except airport reports, was investigated by conducting newspaper, magazine, and internet searches to determine TSSN events. Each event was defined as one event per day, regardless of the time and duration of the day. Information about the airports is given in Table 1. METAR and SPECI reports were obtained from the IOWA Environmental Mesonet website (IOWA 2021). Istanbul Kartal Radiosonde station data were used to determine the change in upper level atmospheric conditions for the region. The closest sounding observation to the time interval in which the TSSN occurred was used. If it occurred almost halfway between two observations, the average values of the two observations were used. All of the sounding data within the specified events were obtained from the University of Wyoming Atmospheric Science's website (University of Wyoming 2021). The indexes used in the determination of the stability of the atmosphere were also obtained from these sounding data. The study area, airports, and radiosonde station are shown in Fig. 1.

In the study, first, the intraday change of TSSN events, their monthly, and annual distributions were determined. Then, the events were classified according to the formation types revealed by Market et al. (2002). Apart from surface meteorological data, other data sets were also needed to perform these classifications. Accordingly, synoptic-scale evaluations were made using the images of the Spinning Enhanced Visible and Infrared Imager (SEVIRI) module of MSG-2 and MSG-3 satellites. Infrared (Channel-9), visible (Channel-321), and airmass satellite images presented at 15-min intervals and 3-km resolution were analyzed (Zhao and Duan 2020). Satellite images were obtained from the Turkish State Meteorological Service (TSMS 2021). In addition, the western Black

Table 1 Information about the airports in the Marmara Region (Source FGA 2021)

Province	Airport	Utilization	ICAO Code	Altitude (m)	Opening data	Latitude–Longitude
Istanbul	Ataturk Airport	International	LTBA	49	1953	40°58′34"N–28°48′51"E
Istanbul	Sabiha Gokcen Airport	International	LTFJ	95	2001	40°53′54"N–29°18′33"E
Istanbul	Samandira Airport	Military	LTBX	123	1988	40°59′34"N–29°12′56"E
Yalova	Taskopru Airport	National-Military	LTBP	13	–	40°41′11"N–29°22′48"E
Kocaeli	Cengiz Topel Airport	International	LTBQ	56	2011	40°44′6"N–30°4′60"E
Tekirdag	Corlu Airport	International	LTBU	31	1998	41°8′18"N–27°55′9"E
Bursa	Yenisehir Airport	International	LTBR	100	2000	40°15′18"N–29°33′45"E
Balikesir	Bandirma Airport	National-Military	LTBG	52	1960	40°19′4"N–27°58′39"E
Balikesir	Kocaseyit Airport	International	LTFD	5	1997	39°33′16"N–27°0′49"E
Balikesir	Balikesir Airport	National-Military	LTBF	104	1998	39°37′9"N–27°55′33"E
Canakkale	Canakkale Airport	National-Military	LTBH	7	1995	40°8′15"N–26°25′36"E

*ICAO, International Civil Aviation Organization

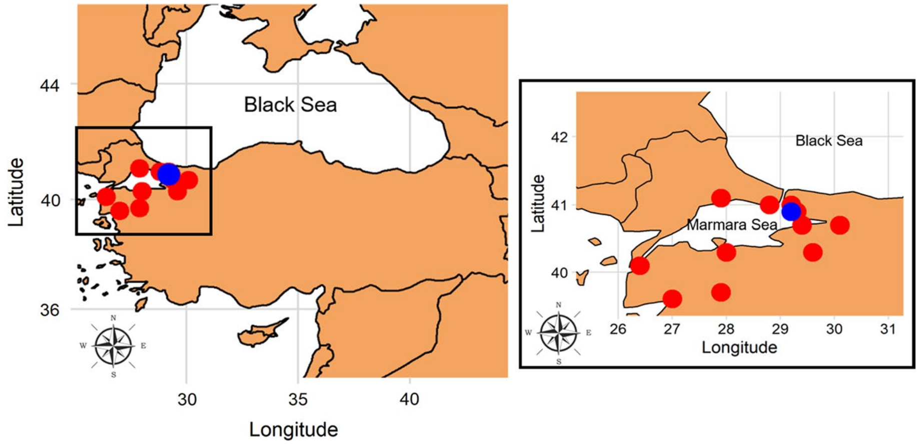

Fig. 1 Study area, location of airports (red dots), and location of Istanbul Kartal radiosonde station (blue dot)

Sea surface temperature data were obtained from the NOAA High-Resolution Blended Analysis dataset (the data with a latitude–longitude resolution of 0.25° × 0.25°) in order to be useful in the detection of events occurring especially with sea-effect (NOAA 2021). For the same purpose, the Woods Hole Oceanographic Institution (WHOI)—Objectively Analyzed Air-Sea Fluxes (OAFlux) dataset was used for sensible and latent heat fluxes (WHOI 2021).

Within the scope of the study, Convective Available Potential Energy (CAPE), Convective Inhibition (CIN), and Bulk Richardson Number (BRN) were analyzed to reveal the stability of the atmosphere in detail. In addition, Lifted Index (LI), Showalter Index (SI), Severe Weather Index (SWEAT), Total Total Index (TTI), and TQ Index (TQI) values were analyzed. Finally, the Pressure of Lifting Condensation Level (LCLP) and Precipitable Water (PWAT) values were calculated. The information about these parameters and indices used to determine the stability of the atmosphere is briefly as follows:

- *CAPE* It is an indicator of atmospheric convection. It is calculated by integrating along the vertical profile of the atmosphere. Its high values are indicative of the instability of the atmosphere. (Lucas et al. 1994; Ye et al. 1998).
- *CIN* It is the negative part of CAPE (Zhang 2003). Its high values are an indication of the stability of the boundary layer.
- *BRN* It is directly related to CAPE. It gives the relationship between CAPE and wind shear vector difference. Its high values indicate the instability of the atmosphere. (Weisman and Klemp 1982).
- *LI* It is the temperature difference between an adiabatically lifted air parcel and the environment at a given pressure. It is used to determine the stability of the lower troposphere. Its low values are an indication of the instability of the atmosphere. (Galway 1956).
- *SWEAT* It is very important for severe weather events. High values of this index are also an indication of high temperature and humidity in the lower atmosphere, the veering of the wind direction with height, the presence of a cooler air pool at the upper levels, and the presence of large vertical wind shear. (Miller 1972).

- *SI* It is a popular severe weather index. It is calculated similarly to LI but less comprehensive. Its low values are an indication of the instability of the atmosphere. (Showalter 1953).
- *TTI* It is calculated using the temperature and dew point temperature values at the 850 and 500 hPa levels. Its high values are indicative of atmospheric instability. (Miller 1972; Pepler and Lamb 1989).
- *TQI* It uses the temperature information at 850 hPa and 700 hPa levels. For low-topped thunderstorm formation, this value must be 12 and above (Henry 2000).
- *LCLP* Higher values indicate that the lower levels of the atmosphere are drier
- *PWAT* It gives the amount of water vapor available for precipitation along the vertical column of the atmosphere in mm.

3 Results

3.1 Frequency and duration of the TSSN events

A total of 19 TSSN events were identified over a 22-year period using aviation reports from 11 airports (Fig. 2a). In addition, reports of thunder and snowfall occurring together were analyzed by looking at newspapers and other online news sites over the internet. Except for the events determined by looking at the airport reports, no extra events were found. Although there is no obvious trend in annual analyses, the observation of six events (almost one third of all events) in 2015 came to the fore. In the study conducted by Market et al (2002) covering the entire United States of America (USA), data from 204 stations over a 30-year period were used, and a total of 191 events

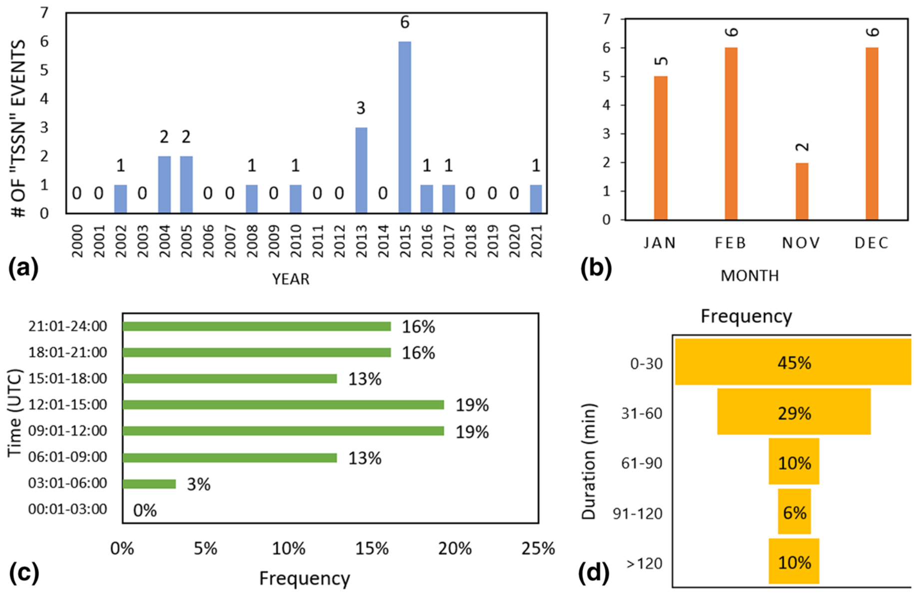

Fig. 2 Annual (**a**), monthly (**b**), intraday (**c**) distributions, and durations (**d**) of TSSN events

were determined based on 3-h reports. Approximately the annual average number of events was around six. Since TSSN event is known as a rare meteorological phenomenon, it is an important result that while the USA is 143 times larger than the Marmara Region in terms of surface area, the events in the USA are only six times more frequent. In monthly analyses, TSSN events were observed in four months of the year, almost similar numbers were observed in winter months, while only two events occurred in November (Fig. 2b). In the USA, events were observed for seven months from October to April, and peak values were reached especially in February and March (Market et al. 2002). Similar results have also been found in the study by Adhikari and Liu (2019). No significant distribution or trend was found in diurnal cycle. However, only 3% of the events were observed between 0000 and 0600 UTC. Maximum frequencies were observed approximately 5–6 h after sunrise until 3 h after sunset (Fig. 2c). Market et al (2002) did not observe a significant trend in intraday changes of TSSN events, whereas Adhikari and Liu (2019) observed maximum frequencies between 1700 and 2400 UTC. The majority of the events (74%) lasted less than an hour, rarely (10%) over 2.5 h (Fig. 2d). Market et al (2002) also determined that one of the longest durations was 5 h at a single station.

3.2 Airport-based surface meteorological analyses

No TSSN events were encountered during the period in 4 of 11 airports (LTBH, LTBQ, LTBR, and LTFD) in the Marmara Region. On 12 January 2015, TSSNs were observed at all seven airports at different times during the day. On this date, at all airports except LTFJ, the TSSN event durations were one hour at the most. At LTFJ, TSSNs lasted 5.5 h in a single day, 4.5 h in the afternoon and 1 h before midnight. Overall, 84% of the events occurred at LTBA and LTFJ, while the rest occurred at other airports excluding these two airports. At three airports (LTBP, LTBU, and LTBX), the TSSN event occurred only on 12 January 2015. In Fig. 3, ranges in the actual/dew point temperature values and relative humidity values at the time of TSSN events at seven airports are given. In Table 2, the average values of meteorological parameters at the time of TSSN events at seven airports are given. As can be seen in Fig. 3, the actual temperature value at airports mostly did not exceed 2 °C, and rarely went below − 1 °C. Considering the event frequencies at LTBA and LTFJ, a wider variation at LTBA and values above 0 °C in almost all events at LTFJ were noted. Market et al. (2002) analyzed the TSSNs and found the mean surface temperatures to be − 1 °C. In similar studies, this value was around 0 °C (Holle et al. 1998; Schultz 1999; Stuart 2001). The dew point temperature values were mostly below 0 °C on average, and oscillation was observed around 0 °C at the LTFJ. In the relative humidity values, the minimum value was seen at LTBA (73%), but mostly it occurred at 87% and above.

In Table 2, it is seen that the average of the actual temperature values for all airports was minimum 0.1 °C and maximum 0.7 °C. The dew point temperature values were slightly above 0 °C at only two airports. While the mean values of wind speeds were close to each other (11.5 kt and 10.6 kt) at LTBA and LTFJ, a high mean value (17.7 kt) was observed at LTBG. Almost all of the prevailing wind directions at the airports were northerly, and most of them are from the north. Average relative humidity values were 90% and above at all airports. While TSSN events were observed at higher station pressure values on average at LTBA compared to LTFJ, no significant difference was found at other airports.

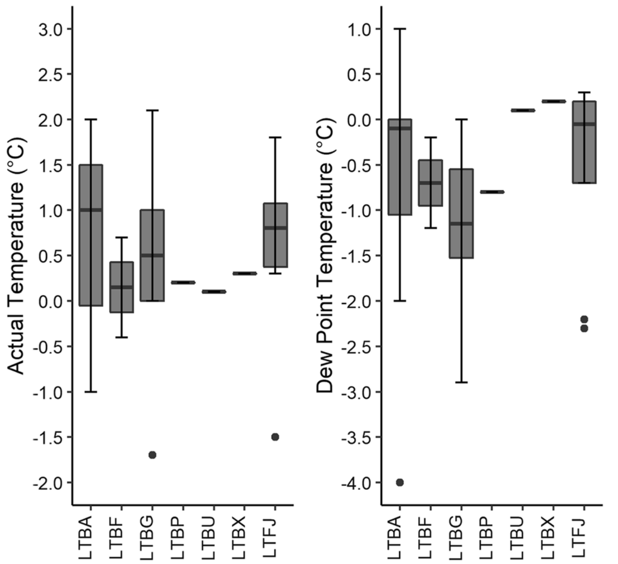

Fig. 3 The variation of actual/dew point temperature and relative humidity values in TSSN events at seven airports

Table 2 Average values of meteorological parameters measured at airports in TSSN events

Airport	T (°C)	Td (°C)	Ws (kt)	Wd	RH (%)	P (hPa)
LTBA	0.7	−0.6	11.5	N	90.0	1028.0
LTBF	0.2	−0.7	11.0	N	94.0	1023.5
LTBG	0.4	−1.2	17.7	N	90.0	1025.7
LTBP	0.2	−0.8	CALM	VRB	93.0	1020.0
LTBU	0.1	0.1	7.0	NW	99.0	1018.0
LTBX	0.3	0.2	9.0	N	99.0	1019.0
LTFJ	0.6	−0.5	10.6	N	92.4	1018.3

CALM, a wind speed less than 1 kt; VRB, wind direction varies by 60 degrees or more

3.3 Analyses of sea surface and upper atmospheric parameters

Air–sea interaction plays an important role in the occurrence of TSSN events. Many processes occur depending on the air–sea interaction. For instance, the source of moisture required for cloud and precipitation formation, buoyancy forces that will carry this moisture to the upper atmospheric levels and initiate convective movements, the presence of convergence to support convective vertical development, advections to carry cold air within the cloud and lower atmospheric levels, etc. In this study, the average daily sea surface temperatures (SSTs) for the western Black Sea were obtained separately for all TSSN events, and the temperature differences between the upper atmospheric levels (850 and 700 hPa) and SS were analyzed (Fig. 4). In addition, average and maximum values of sensible and latent heat fluxes for all events were also investigated.

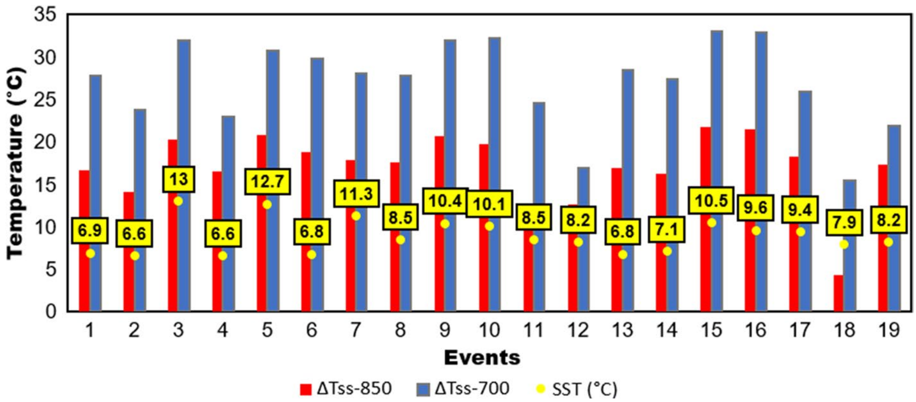

Fig. 4 The red and blue bar graphs show $\Delta T_{SS\text{-}850}$ and $\Delta T_{SS\text{-}700}$ for the western Black Sea, respectively. The values in the boxes determined by the yellow dots give the daily average SST value for each TSSN event

The average SST value for all TSSN events was 8.9 °C. The lowest value observed was 6.6 °C, the highest was 13.0 °C. However, the most important thing here is to determine the temperature difference between upper atmospheric levels and SS. Accordingly, $\Delta T_{SS\text{-}850}$ and $\Delta T_{SS\text{-}700}$ values were analyzed for all events. Higher values increase the temperature gradient in the region, support the necessary lifting mechanisms to carry more heat and moisture fluxes from the SS to the upper atmospheric levels, and as a result, a more unstable atmosphere occurs due to increased convection. In studies on lake/sea effect snowfalls (LES/SES) in the literature, threshold values were generally used for $\Delta T_{SS\text{-}850}$ and $\Delta T_{SS\text{-}700}$ so that heat and moisture fluxes over water bodies could initiate cloud band formations at higher atmospheric levels. These values were 13.0 °C (Holroyd 1971; Niziol et al. 1995; Kunkel et al. 2002; Laird et al. 2009; Yavuz et al. 2021b, 2022b) and 17.0 °C (Niziol 1987; Carpenter 1993; Steenburgh et al. 2000), respectively. Values above these thresholds both strengthen cloud band structures and increase the amount of precipitation. However, when these conditions occur, it has been stated that an inversion layer that limits the convective movements at higher atmospheric levels must also occur (Pettersen 1956; Rothrock 1969; Hjelmfelt 1990; Reinking et al. 1993; Yavuz et al. 2021c, 2022c). At the same time, the longer the distance (fetch distance) that the cold air parcel travels on the relatively warm water surfaces, the more the heat and moisture fluxes pass through the water bodies to the upper atmosphere, which supports the instability (Jiusto and Kaplan 1972; Kristovich and Laird 1998; Fujisaki-Manome et al. 2017). It is also important that the directional wind shear in the convective boundary layer is less than 60° in the formation of cloud band structures and in the determination of their trajectories (Carpenter 1993; Steenburgh and Onton 2001; Laird et al. 2003; Laird and Kristovich 2004). In this study, the $\Delta T_{SS\text{-}850}$ value was calculated as an average of 17.0 °C for all events, and the $\Delta T_{SS\text{-}700}$ value was calculated as an average of 27.0 °C. The $\Delta T_{SS\text{-}850}$ value was found to be minimum 4.3 °C (but the smallest value after this value was 10.2 °C), and the highest value was 21.8 °C. The minimum value for $\Delta T_{SS\text{-}700}$ was found to be 15.4 °C and the maximum value as 33.0 °C (Fig. 4). Inversion layers were detected at various atmospheric levels in all sounding data analyzed within 19 events. The majority of these layers were located between 800–650 hPa (not shown). Heat and moisture fluxes are very important as they destabilize lower atmospheric levels over water bodies (Gerbush et al. 2008). These fluxes, which are necessary for the formation of the convective layer, have different effects depending on the shape of the water body, the presence of synoptic- and large-scale systems, and the wind conditions at the surface of the water bodies (Scott and Sousounis 2001; Markowski and Richardson 2010). Sensible and latent heat fluxes in LES events varied in the range of 50–150 W m^{-2} (Lang et al. 2018), these values were observed in the range of 200–500 W m^{-2} when strong bands and heavy snowfalls occur due to increased instability and convection (Sousounis and Mann 2000). In this study, the average values of sensible and latent heat fluxes were 140.4 W m^{-2} and 161.2 W m^{-2}, respectively. A minimum of 20 W m^{-2} and a maximum of 306 W m^{-2} were determined in the sensible heat flux. A minimum of 83 W m^{-2} and a maximum of 352 W m^{-2} were observed in the latent heat flux (Fig. 5). In the final analysis made in this section, it was determined that 84% of the wind directions from surface level to 700 hPa level were veering (anticyclonic turning of wind direction with height). Similarly, Market et al. (2006) determined that veering was dominant in the sounding analyses for TSSNs.

3.4 Formation types of the TSSN events

In this study, initially the aim was to complete an analysis similar to the classification of TSSN events according to the formation types made by Market et al. (2002), but the classification was slightly different. The most important reason for the difference in classification was that 17 of 19 TSSN events had a distinctly SES mechanism. For this reason, it was determined whether SES events occur singularly or together with synoptic-scale systems (such as: cyclone; front; trough).

SESs were observed in 17 of 19 events, and the other two SES-independent events also occurred within the frontal and cyclone effects. In general, cyclones were observed on and in the immediate vicinity of the study area in 10 of 19 events. Similarly, in 12 of the 19 events, a front was observed on and in the immediate vicinity of the study area. Therefore, the SES that occurred after the frontal and cyclone transitions was effective as sea-enhanced snowfall. This increased both the intensity of the SES bands and the total amount of snowfall. Considering the analyses made in Sect. 3.3, it was determined that the requirements for the SES mechanism were more than met in most of the cases, in terms of air–sea interaction. In the classification made by Market et al. (2002), almost half of the TSSN events took place in the cyclone class. In this study, most of the events took place with the

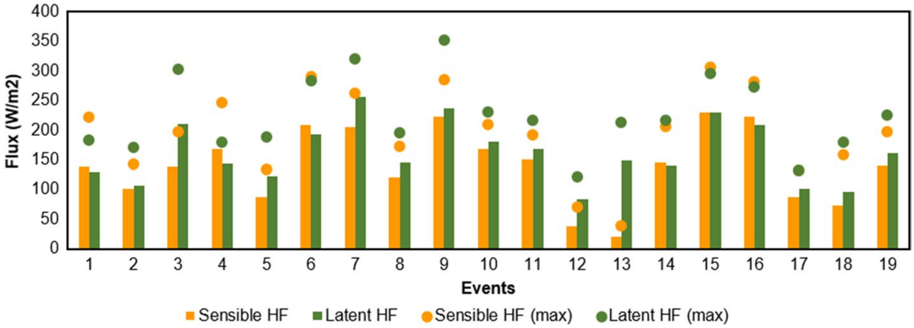

Fig. 5 Orange and green bars show sensible and latent heat fluxes, respectively. Dots of the same color on the bars also give the maximum values of the both heat fluxes

SES mechanism, and more than half of them occurred after the transition of cyclone and frontal systems.

3.5 Atmospheric stability analyses

In this section, atmospheric stability indexes and analyses of some sounding parameters were carried out. The information about the values of these indexes and parameters, in which intervals, and what they mean is given in Table 3. Each parameter has its own distinct value range. In addition, many parameters not only give information about the stability of the atmosphere, but also provide information about the severity and distribution of TSs, whether the necessary conditions for the formation of supercell and multicell are met, and the probability and severity of tornado formation. No criteria were found for LCLP, but it was still included in the table. Because this parameter provides important information about the moisture content in the lower troposphere. Similarly, the PWAT value gives information about the moisture content, not about the stability of the atmosphere. In the analyses, in addition to the PWAT values, the relative humidity (RH) values at 850- and 700-hPa levels were also analysed.

In terms of representing the vertical profile of the atmosphere, the Skew-T Log-P diagram at 1200 UTC on 12 January 2015, when the TSSN events occurred at all seven airports, is given in Fig. 6. The TSSN event occurred longest at LTFJ (285 min) and shortest at LTBA (38 min). In the presence of TSSN events, the average relative humidity at airports was 96%. As can be seen in the diagram, the surface level air temperature is around 0 °C. The actual and dew point temperature lines are nearly overlapped from surface level to about 375 hPa level. The parcel lapse rate usually starts from the surface in the warm season. This may not be the case in the cold season. Elevated convection can be observed in TSSN events. Most atmospheric stability indexes cannot make accurate predictions due to elevated convection. In this diagram, the atmosphere is stable below 600 hPa, and above that is looks unstable, so any convection leading to the lightning and thunder is elevated above the stable layer (an inversion layer). It is also seen that there is a serious cooling above from the 300 hPa level. This is an indication that a large-scale system may exist. The fact that the wind veering with height at this level indicates that there may be a warm advection layer here.

In parallel with the information in the literature for CAPE values (Sect. 1), much lower CAPE values were observed in winter TSs compared to summer TSs. In the TS analyses conducted by Özdemir et al. (2017) at LTBA within the 2008–2013 period, the annual average CAPE values in the winter period varied between 0 W m^{-2} and 30.6 W m^{-2}. Similarly, in the same study, CIN values were found to be between −75.5 W m^{-2} and 0 W m^{-2} on annual averages. In this study, results similar to those in the literature were obtained in all TSSN events, except for Event-14. In Event 14, it was determined that the atmosphere was marginally unstable in terms of the CAPE value. A similar structure was observed in BRN values as well as CAPE values. Event 14 was the only event where buoyant forces dominated vertical shear, and a multicell structure was most likely to be observed (Table 4). Therefore, although these three sounding parameters gave good results for summer TSs, they were not successful for winter TSs.

In the atmospheric stability indexes, some indexes were almost unsuccessful, while clear information about the instability of the atmosphere could be obtained from some of them. While LI only showed that the atmosphere was very unstable in Event 14, TS and tornadoes were possible, it could not make a similar determination for other events. The

Table 3 The ranges and meanings of atmospheric stability indexes' values and values of some sounding parameters (2021). Source: NWS

	Severe weather activity
CAPE	"CAPE < 300, stable"
	"300 < CAPE < 1000, marginally unstable"
	"1000 < CAPE < 2500, moderately unstable"
	"CAPE > 2500, very to extremely unstable"
CIN	"CIN < 100, potential instability"
	"100 < CIN < 200, marginally stable"
	"200 < CIN < 300, moderately stable"
	"CIN > 400, very stable"
BRN	"BRN < 10, much more shear than buoyancy, TSs unlikely"
	"10 < BRN < 45, balance between shear and buoyancy, supercells possible"
	"BRN > 45, buoyancy dominates over shear, multicells more likely"
LI	LI > 2, stable
	"0 < LI < 2, weak convection, TSs possible with other source of lift"
	" – 2 < LI < 0, TSs possible, trigger needed, marginally unstable"
	" – 4 < LI < – 2, TSs probable, moderately unstable"
	"LI < – 4, severe TSs possible, tornado possible, very unstable"
SWEAT	"SWEAT < 150, TSs unlikely"
	"150 < SWEAT < 300, slight severe, no severe TSs"
	"300 < SWEAT < 400, severe TSs possible"
	"SWEAT > 400, severe TSs probable, tornadoes possible"
SI	SI > 3, stable
	"1 < SI < 3, rain showers, thundershowers possible with other source of lift"
	" – 2 < SI < 1, TSs possible, marginally unstable"
	" – 3 < LI < – 2, TSs probable, moderately unstable"
	" – 6 < SI < – 4, severe TSs, very unstable"
	" SI < – 6, strong/severe TSs more probable, tornado possible, extreme unstable"
TQI	"44–45, isolated TSs
	"46–47, scattered moderate TSs,
	"48–49, scattered severe TSs
	"50–51, scattered severe TSs, isolated tornadoes"
	"52–55, scattered to numerous TSs, few tornadoes"
	TTI > 55, numerous TSs, scattered tornadoes Low-topped thunderstorms possible with the threshold value of 12
LCLP	"No scale was found. High values indicate how dry the atmosphere is up to that level"
	"A low LCLP (closer to surface) increases tornadogenesis"
PWAT	"PWAT < 12.7 mm, very low moisture content"
	"12.8 < PWAT < 31.8 mm, low moisture content"
	"31.8 < PWAT < 44.5 mm, moderate moisture content"
	"44.5 < PWAT < 50.8 mm, high moisture content"

SWEAT index showed that slight severe conditions were present in three events and not a severe TS, that severe TS could occur in one event, and finally, severe TS and tornadoes were possible for Event 14. SI showed that thundershowers were possible in an event if

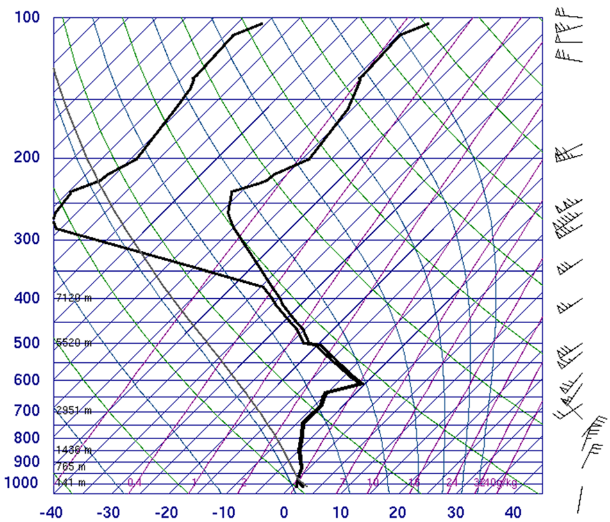

Fig. 6 Skew-T Log-P diagram at 1200 UTC on 12 January 2015 (Source: University of Wyoming 2021)

Table 4 Atmospheric stability indexes and some parameters that give information about the vertical atmosphere structure

	CAPE	CIN	BRN	LI	SWEAT	SI	TTI	TQI	LCLP	PWAT	RH_{850}	RH_{700}
Event-1	0	**0**	0	16.2	106	15	34.4	**14.1**	938	8.2	85	76
Event-2	0	**0**	0	9.2	**155**	7	**49.6**	**12.5**	892	8	88	80
Event-3	5	**−8**	0.3	11.1	63	11.6	**51.2**	**11.6**	938	6.3	85	10
Event-4	0	**0**	0	5	91	5.5	**51.2**	5.9	893	6.3	62	13
Event-5	7	**0**	0.3	7.1	109	8.6	**48**	8.6	942	5.8	75	65
Event-6	0	**0**	0	7.3	97	7.6	**48.9**	10.9	894	6.1	78	75
Event-7	20	**−24**	0.4	11.7	134	12	40.2	**13.9**	946	7	81	22
Event-8	0	**0**	0	17.7	142	14.1	34.1	**11.6**	979	17.2	98	98
Event-9	0	**0**	0	10	124	9.2	**45.8**	**12.9**	950	8.2	87	78
Event-10	12	**−1**	0.9	7.7	79	9.9	**49.5**	**15.6**	986	6.9	96	77
Event-11	0	**0**	0	3	**168**	3.6	**54.8**	**19.0**	849	5.6	62	28
Event-12	0	**0**	0	10	114	10	43.3	5.5	936	9.6	89	81
Event-13	3	**−12**	0.3	4.9	**302**	**1**	**61.7**	**14.1**	953	8.6	89	81
Event-14	**501**	**−207**	**67.2**	**−9.1**	**495**	**−4.7**	**69.8**	**14.5**	769	14.6	69	83
Event-15	0	**0**	0	16.3	65	16	31.8	**14.1**	879	5.9	79	17
Event-16	0	**0**	0	12.7	74	12.7	39.6	**15.3**	973	6.9	88	84
Event-17	20	**−7**	2	14.9	83	15.8	32.6	8.0	921	7	81	79
Event-18	11	**−1**	5.9	10.9	50	9.6	**44.3**	**16.0**	956	8.5	85	79
Event-19	0	**0**	0	4.9	**223**	3.2	**51**	2.1	931	18.5	75	91

In some values, bold font was used to express important values for each TSSN event

there was another source of lift, and for Event 14, extreme unstable atmospheric conditions were present and severe TSs and tornadoes could be seen. The TTI was the second most successful index in revealing the instability of the atmosphere among the indexes. It showed that in 12 of the 19 TSSN events, unstable atmospheric conditions were present. In one of these, it was found that TSs from scattered to enormous would occur and it was possible to see a few tornadoes. It also showed that it was quite possible to observe enormous TSs and scattered tornadoes for Events 13 and 14. Finally, the TQI was the most successful index to reveal the instability of the atmosphere. This index, which is calculated depending on the air temperature and dew point temperature at 850 hPa and the air temperature at 700 hPa, is free from surface level characteristics and daily changes in the characteristics of the layer close to the surface.

LCLP indicates the pressure level at which the LCL value was found. This sounding parameter gives important information about the moisture content in the lower atmosphere. In almost all TSSN events, these levels were determined to vary between 840 and 986 hPa (with the exception of Event 14, 768.9 hPa was detected in that event). Therefore, the lower parts of the atmosphere were not very dry in TSSN events. In PWAT values, mostly very low and low moisture content values were determined. However, this value does not directly look at the humidity for the lower levels of the troposphere, but gives information about the precipitable water content in the entire sounding. A deep column of water vapor is not expected for cold season events, so the same PWAT values confined to low levels are better than it being distributed through a depth. For this reason, humidity information at 850 hPa and 700 hPa levels was also examined. For TSSN events, the average relative humidity value at the 850 hPa level was 81.7%, and this value was 64.1% at the 700 hPa level (Table 4). These values indicated that the lower tropospheric levels near the ground (especially around 850 hPa) were rich in moisture content, as observed LCL pressure levels.

4 Discussion and conclusions

In this study, the temporal analyses of TSSN events over a 22-year period were made based on airport reports and the atmospheric conditions in which they occurred were investigated. Such a short-term and rare event has several serious negative effects, especially in terms of aviation activities. In most of the events, it was found that the horizontal visibility decreased drastically when TSSN was observed. In addition, high wind speeds, which often have gust, have been the common adverse condition observed at all airports where TSSN was observed. TSSN events were mostly observed in restricted areas and for a short time (0–1 h). These events were observed only in winter and in November (only two events) during the period. Considering the intraday distributions, no trend was found as in Market et al. (2002). However, very few TSSN events were observed from midnight to sunrise. There are two important points for TS coding at airports. One of them is the hearing of the thunder by the observer and the other is the observation of the lightning. For this reason, it was not thought that less TSSN occurrence in the hours from midnight to sunrise is an observation deficiency or error, but on the contrary, it is known that better observation is made during night hours.

It was determined that in the airport reports that TSSN events were observed in the range of −1 °C and 2 °C. Market et al. (2002) found this value to be around -1 °C, and Schultz (1999) and Stuart (2001) found it around 0 °C. In this study, actual temperature values close to 2 °C were rarely observed, but mostly there were variations around 0 °C. The high relative humidity values (90% and above) observed in these reports indicate that the humidity required for unstable atmospheric conditions and convective movements was available. In addition, when TSSN events were observed, at almost all airports, the wind direction was northerly. This is directly proportional to the fact that the systems that bring precipitation in the Marmara Region, especially in winter, enter from the north. Most of the heavy snowfall caused by the synoptic-scale systems (long-wave troughs, short-wave troughs, fronts, low pressure centres, sea-effect mechanisms) in the region is dominated by northern flows. It was not a coincidence that 6 of the 19 events during the period were observed in 2015, and that one event was detected at different times during the day at all airports where TSSN was observed on 12 January in the same year. It was related to the existence of four different SES systems in total throughout the region that year, and the formation of intense and sea-enhanced snow band structures as a result of almost all of these systems being supported by synoptic-scale systems (mostly after cyclone and frontal passages) (Yavuz et al. 2021b).

The classification of TSSN events according to their formation was similar to the classification made by Market et al. (2002), but the dominance of a single class (SES mechanism) was decisive throughout the period. Sea-effect or sea-enhanced snow mechanisms were observed in 17 of 19 events. On the other hand, Market et al. (2002) approximately found 10% of the TSSN times when the LES mechanism was effective. Air–sea interaction is an important parameter in SES mechanisms, which occur at the meso-scale and exacerbate from time to time with synoptic-scale systems. From this point of view, TSSN and SES event mechanisms are similar to each other due to the atmospheric conditions they require. The arctic and polar origin cold air parcel transported over the western Black Sea during the long fetch (150–600 km) distance could easily meet the humidity requirement (heat and moisture fluxes) for both TS and SES in most of the events analyzed during the period. The average values of $\Delta T_{SS\text{-}850}$ and $\Delta T_{SS\text{-}700}$ for all TSSN events were observed as 17 °C and 27 °C, respectively. Due to these high temperature differences between the upper atmosphere and the SS, heat and moisture fluxes from the SS to the upper atmosphere were easily transferred, when the long fetch distance is also taken into account. It is known that sensible and latent heat flux values are directly proportional to the aforementioned temperature differences, and it was determined in this study as well. These high heat and moisture fluxes were caused by or contributed to the formation of high humidity, unstable atmospheric conditions, lifting mechanism, and additionally directional wind shear along the convective boundary layer required for the TS mechanisms. Similar to the result found by Market et al. (2006) in the sounding analyses, veering movements were observed in most cases (84%). In addition, cold air advections were observed in most of the sounding analyses.

Although CAPE values are a suitable analysis parameter to evaluate summer TSs, it is the opposite for winter TSs. Almost all of the CAPE values (except for one event) seem to have stable atmospheric conditions during TSSN events. The fact that TSSN events usually occur as a result from slantwise convection causes the CAPE values to be low. The potential for this is not captured by CAPE as the buoyancy gradient does not exist in the vertical. TTI was the index that made the second most successful prediction in the analyses made by considering the atmospheric stability indexes. There are several reasons for this. TTI, which is used as a measure of TS potential, consists of two basic components: vertical totals (VT) and Cross Totals (CT). VT takes into account lapse rate and static stability between 850- and 500-hPa, while CT takes into account the lower-level moisture throughout 850-hPa. The higher the value of these components, the higher the index value. Increasing values of the index also show that the TS potential is increasing. There are also some disadvantages of the index. Since only parameters in the range of 850 and 500 hPa are used, it does not take into account inversion layers, and moist or dry layers that exist below the 850 hPa level. In addition to these

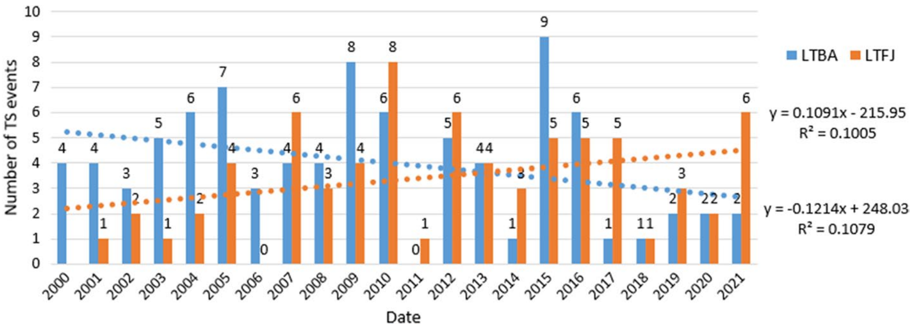

Fig. 7 Total number of TS events that occurred in January, February, November, and December at LTBA and LTFJ from 2000 to 2021

disadvantages of the TTI, directional wind shear, which is critical in the formation of TS, is an important parameter that the index does not take into account. It is also important that the study area should be below the 850-hPa level for the index to be usable. All of the airports analyzed in this study are located at altitudes close to sea level. In addition, analyses were carried out considering the airport reports and sounding data on directional wind shear, and it was observed in these analyses that sufficient conditions for TS were created. On the other hand, it was known that the moisture content 850 hPa and below was quite sufficient according to the analysis results obtained from both the sounding data and the airport reports. Finally, in the sounding analyses made, inversion layers were detected in only a few observations at 850 hPa and below, but these also had very low thickness values (45–130 m). When analyzing TTI values, it was seen that high consistency estimates can be made for TSSN with the additional analyses to be made for the above-mentioned 850-hPa and lower levels. Besides the TTI, the TQI has the most successful performance among indexes. One of the most important factors that makes this index successful is that it takes into account the instability in the range of 700–500 hPa levels. Although the TQI is more successful in deeply unstable warm season convective environments, it was successful in detecting the TSSN events considered in this study.

For the two airports (LTBA and LTFJ) where the majority of TSSN events occurred, analyses of TS events occurring in January, February, November, and December were carried out within the study period (Fig. 7). As the TSSN events within the period occurred only in these four months, analyses of the TS events were performed for similar months. An increasing linear trend at LTFJ and a decreasing linear trend at LTBA were noted. However, a similar trend was not observed both between cold-season TS and TSSN events, and between airports located in two different regions in the same province. Therefore, it is necessary to conduct a comprehensive study on the forecast of cold-season TS and TSSN events for the region.

Acknowledgements This work is funded by the Turkish Science Foundation (TUBITAK) with Grant Number 1059B142000051. The authors would like to thank the Turkish State Meteorological Service for the data used in this study.

Author contributions VY: Conceptualization, Introduction, Methodology, Formal analysis, Writing—Original draft preparation, Writing, Reviewing and Editing. ARL: Conceptualization, Supervision, Writing, Reviewing and Editing. NIF: Conceptualization, Supervision, Writing, Reviewing and Editing. AD: Conceptualization, Supervision, Writing, Reviewing and Editing.

Funding The work is funded by the Turkish Science Foundation (TUBITAK) with Grant Number 1059B142000051.

Availability of data and material Not applicable.

Code availability Not applicable.

Declarations

Conflict of interest The authors have no conflict of interest to declare that are relevant to the content of this article.

Consent for publication The authors confirm that the study is original and abide within the regulations for publication.

Consent to participate Not applicable.

Ethical approval Not applicable.

References

Ackerman SA, Knox JA (2002) Meteorology: understanding the atmosphere: Brooks
Adhikari A, Liu C (2019) Geographical distribution of thundersnow events and their properties from GPM Ku-band radar. J Geophy Res Atmos 124(4):2031–2048. https://doi.org/10.1029/2018JD028839
Bech J, Pineda N, Rigo T, Aran M (2013) Remote sensing analysis of a mediterranean thundersnow and low-altitude heavy snowfall event. Atmos Res 123:305–322. https://doi.org/10.1016/j.atmosres.2012.06.021
Carpenter DM (1993) The lake effect of the great lake: overview and forecast problems. Wea Forecast 8:181–193
Cherington M (2001) Lightning injuries in sports: situations to avoid. Sports Med 31(4):301–308. https://doi.org/10.2165/00007256-200131040-00004
Colman BR (1990a) Thunderstorms above frontal surfaces in environments without positive CAPE. Part i: climatology. Mon Wea Rev 118(5):1103–1122
Colman BR (1990) Thunderstorms above frontal surfaces in environments without positive CAPE. Part II: organization and instability mechanisms. Mon Wea Rev 118(5):1123–1144
Crowe C, Market P, Pettegrew B, Melick C, Podzimek J (2006) An investigation of thundersnow and deep snow accumulations. Geophys Res Lett 33(24):L24812. https://doi.org/10.1029/2006GL028214
Curran JT, Pearson AD (1971) Proximity soundings for thunderstorms with snow preprints, seventh Conference on severe local storms. American meteorological society Kansas City, MO. pp 118–119.
Doswell CA III, Evans JS (2003) Proximity sounding analysis for derechos and supercells: an assessment of similarities and differences. Atmos Res 67–68:117–133. https://doi.org/10.1016/S0169-8095(03)00047-4
Dunya (2015) Severe storm affected flights at Sabiha Gokçen Airport. https://www.dunya.com/gundem/siddetli-ruzgar-ucak-seferlerini-de-etkiledi-haberi-268222. Accessed 21 November 2021
Elkins HA (1987) Thunderstorms with snow: a comprehensive, empirical study of their occurrence, development and structure. M. S. Thesis, Saint Louis University, p 79
FGA (2021) Future Generation Aviation: airports in Turkey. http://www.tr.auto-gyro.com/sayfa/ucus-hazirligi/turkiye-havaalanlari.html Accessed 23 November 2021
Fujisaki-Manome A, Fitzpatrick LE, Gronewold AD, Anderson EJ, Lofgren BM, Spence C, Chen J, Shao C, Wright DM, Xıao C (2017) Turbulent heat fluxes during an extreme lake-effect snow event. J Hydrometeorolo 18(12):3145–3163. https://doi.org/10.1175/JHM-D-17-0062.1
Galway JG (1956) The lifted index as a predictor of latent instability. Bull Amer Meteor Soc 43:528–529. https://doi.org/10.1175/1520-0477-37.10.528
GDSAA (2021) General Directorate of State Airports Authority, Republic of Turkey ministry of transport and infrastructure: Airport information. https://www.dhmi.gov.tr/Sayfalar/HavaLimanlari.aspx Accessed 29 November 2021

Gerbush MR, Kristovich DAR, Laird NF (2008) Mesoscale boundary layer and heat flux variations over pack ice-covered Lake Erie. J Appl Meteor Climatol 47(2):668–682. https://doi.org/10.1175/2007JAMC1479.1

Halcomb CE, Market PS (2003) Forcing, instability, and equivalent potential vorticity in a midwestern U.S. convective snowstorm. Meteorol Appl 10:273–280. https://doi.org/10.1017/S1350482703003074

Henry NL (2000) A static stability index for low-topped convection. Wea Forecast 15(2):246–254. https://doi.org/10.1175/1520-0434(2000)015%3c0246:ASSIFL%3e2.0.CO;2

Hjelmfelt MR (1990) Numerical study of the influence of environmental conditions on lake-effect snowstorms on Lake Michigan. Mon Wea Rev 118:138–150. https://doi.org/10.1175/1520-0493(1990)118%3C0138:NSOTIO%3E2.0.CO;2

Holle RL, Cortinas JV, Robbins CC (1998) Winter thunderstorms in the United States. Preprints, 16th Conf. on weather analysis and forecasting, phoenix, AZ, Amer Meteor Soc 298–300

Holroyd EW III (1971) Lake-effect cloud bands as seen from weather satellites. J Atmos Sci 28:1165–1170. https://doi.org/10.1175/1520-0469(1971)028%3c1165:LECBAS%3e2.0.CO;2

IOWA (2021) Environmental mesonet: ASOS-AWOS-METAR data. https://mesonet.agron.iastate.edu/request/download.phtml. Accessed 29 November 2021

Jiusto JE, Kaplan ML (1972) Snowfall from lake-effect storms. Mon Wea Rev 100(1):62–66. https://doi.org/10.1175/1520-0493(1972)100%3c0062:SFLS%3e2.3.CO;2

Kristovich DAR, Laird NF (1998) Observations of widespread lake-effect cloudiness: influences of lake surface temperature and upwind conditions. Wea Forecast 13(3):811–821. https://doi.org/10.1175/15200434(1998)013%3c0811:OOWLEC%3e2.0.CO;2

Kumijan MR, Dierling W (2015) Analysis of thundersnow storms over northern Colorado. Wea Forecast 30(6):1469–1490. https://doi.org/10.1175/WAF-D-15-0007.1

Kunkel KE, Wescott NE, Kristovich DAR (2002) Assessment of potential effects of climate change on heavy lake-effect snowstorms near lake-Erie. J Gt Lakes Res 28:521–536. https://doi.org/10.1016/S0380-1330(02)70603-5

Laird NF, Walsh JE, Kristovich DAR (2003) Model simulations examining the relationship of lake-effect morphology to lake shape, wind direction, and wind speed. Mon Wea Rev 131(9):2102–2111

Laird NF, Kristovich DAR (2004) Comparison of observations with idealized model results for a method to resolve winter lake-effect mesoscale morphology. Mon Wea Rev 132:10931103

Laird NF, Desrochers J, Payer M (2009) Climatology of lake-effect precipitation events over lake Champlain. J Appl Meteorol 48:232–250. https://doi.org/10.1175/2008JAMC1923.1

Lang CE, McDonald JM, Gaudet L, Doeblin D, Jones EA, Laird NF (2018) The influence of a lake-to-lake connection from Lake Huron on the lake-effect snowfall in the vicinity of lake Ontario. J Appl Meteor 57(7):1423–1439. https://doi.org/10.1175/JAMC-D-17-0225.1

Lucas C, Zipser EJ, LeMone MA (1994) Convective available potential energy in the environment of oceanic and continental clouds: correction and comments. J Atmos Sci 51(24):3829–3830. https://doi.org/10.1175/1520-0469(1994)051%3c3829:CAPEIT%3e2.0.CO;2

Market PS, Halcomb CE, Ebert RL (2002) A Climatology of thundersnow events over the contiguous United States. Wea Forecast 17(6):1290–1295. https://doi.org/10.1175/1520-0434(2002)017%3c1290:ACOTEO%3e2.0.CO;2

Market PS, Oravetz AM, Gaede D et al (2006) Proximity soundings of thundersnow in the central United States. J Geophys Res. https://doi.org/10.1029/2006JD007061

Market PS, Ebert-Cripe RL, Bodner M (2007) Case study of a longlived thundersnow event. Nat Weather Dig 31:103–120

Mäkelä A, Saltikoff E, Julkunen J, Juga I, Gregow E, Niemelä S (2013) Cold-season thunderstorms in Finland and their effect on aviation safety. Bull of Amer Meteor Soc 94(6):847–858. https://doi.org/10.1175/BAMS-D-12-00039.1

Markowski P, Richardson Y (2010) Mesoscale meteorology in midlatitudes. Wiley-Blackwell, Chichester, p 407

Miller RC (1972) Notes on the analysis of severe storm forecasting procedures of the air force global weather center AFGWC Tech Rep 200. Air Weather Service, Scott AFB, IL

Munzar J, Franc M (2003) Winter thunderstorms in central Europe in the past and the present. Atmos Res 67–68:501–515. https://doi.org/10.1016/S0169-8095(03)00062-0

Niziol TA (1987) Operational forecasting of lake effect snowfall in western and central New York. Weather Forecast 2(4):310–321. https://doi.org/10.1175/1520-0434(1987)002%3C0310:OFOLES%3E2.0.CO;2

Niziol TA, Snyder W, Waldstreicher J (1995) Winter weather forecasting throughout the eastern United States. Part IV: lake effect snow. Wea Forecast 10:61–77. https://doi.org/10.1175/1520-0434(1995)010%3c0061:WWFTTE%3e2.0.CO;2

NOAA (2021) National Oceanic and Atmospheric Administration: NCEP/NCAR reanalysis II. https://psl.noaa.gov/data/gridded/data.ncep.reanalysis.pressure.html.Accessed 7 November 2021
NWS (2021) National Weather Service: Definition of atmospheric variables, atmospheric stability indicies. https://www.weather.gov/ffc/gloss2. Accessed 7 October 2021
Özdemir ET, Deniz A, Sezen İ, Aslan Z, Yavuz V (2017) Investigation of thunderstorms over Ataturk International Airport (LTBA) Istanbul. Mausam 68(1):175–180
Özdemir ET, Yavuz V, Deniz A, Karan H, Kartal M, Kent S (2019) Squall line over antalya: a case study of the events of 25 October 2014. Weather 74(S1):S1–S6. https://doi.org/10.1002/wea.3459
Özdemir ET (2021) A Case study of a multicell severe convective storm in Ankara, Turkey. Pure Appl Geophys 178:4107–4126. https://doi.org/10.1007/s00024-021-02795-y
Pepler RA, Lamb PJ (1989) Tropospheric static stability and central north American growing season rainfall. Mon Wea Rev 117(6):1156–1180. https://doi.org/10.1175/1520-0493(1989)117%3c1156:TSSACN%3e2.0.CO;2
Pettersen S (1956) Weather analysis and forecasting:, vol II. McGraw-Hill, Weather and Weather Systems, p 266
Reinking RF, Caiazza R, Kropfli RA, Orr BW, Martner BE, Niziol TA, Byrd GP, Penc RS, Zamora RJ, Snider JB, Ballentine RJ, Stamm AJ, Bedford CD, Joe P, Koscielny AJ (1993) The Lake-Ontario winter storms (LOWS) project. Bull Amer Meteor Soc 74(10):1828–1849
Rothrock HJ (1969) An aid in forecasting significant lake snows. Tech Memo WBTM CR-30, National weather service central the region, p 16
Schultz DM (1999) Lake-effect snowstorms in northern utah and western New York with and without lightning. Wea Forecast 14(6):1023–1031. https://doi.org/10.1175/1520-0434(1999)014%3c1023:LESINU%3e2.0.CO;2
Schultz DM, Vavrek RJ (2009) An overview of thundersnow. Weather 64(10):274–277. https://doi.org/10.1002/wea.376
Scott CPJ, Sousounis PJ (2001) The utility of additional soundings for forecasting lake-effect snow in the great lakes region. Wea Forecast 16(4):448–462
Showalter AK (1953) A stability index for forecasting thunderstorms. Bull Amer Meteor Soc 34(6):250–252. https://doi.org/10.1175/1520-0477-34.6.250
Sousounis PJ, Mann GE (2000) Lake-aggregate mesoscale disturbances. Part V: Impacts on lake-effect precipitation. Mon Wea Rev 128(3):728–745
Steenburgh WJ, Halvorson SF, Onton DJ (2000) Climatology of lake-effect snowstorms of the great Salt Lake. Mon Wea Rev 128:709–727. https://doi.org/10.1175/1520-0493(2000)128%3C0709:COLESO%3E2.0.CO;2
Steenburgh WJ, Onton DJ (2001) Multiscale Analysis of the 7 December 1998 great Salt lake-effect Snowstorm. Mon Wea Rev 129(6):1296–1317. https://doi.org/10.1175/1520-0493(2001)129%3c1296:MAOTDG%3e2.0.CO;2
Stuart NA (2001) Multi-dimensional analysis of an extreme thundersnow event during the 30 December 2000 snowstorm. In 18th Conference on Weather Analysis and Forecasting, Fort Lauderdale, FL, Amer Meteor Soc 18:223–226.
TSMS (2021) Turkish State Meteorological Service. http://www.mgm.gov.tr. Accessed 24 December 2021University of Wyoming (2021) Upper-level atmospheric charts. http://weather.uwyo.edu/upperair/sounding.html. Accessed 9 October 2021
Wahiduzzaman M, Ali MA, Luo JJ et al (2022) Effects of convective available potential energy, temperature and humidity on the variability of thunderstorm frequency over Bangladesh. Theor Appl Climatol 147:325–346. https://doi.org/10.1007/s00704-021-03833-4
Weisman ML, Klemp JB (1982) The dependence of numerically simulated convective storms on vertical wind shear and buoyancy. Mon Wea Rev 110:504–520. https://doi.org/10.1175/1520-0493(1982)110%3c0504:TDONSC%3e2.0.CO;2
WHOI (2021) Woods Hole Oceanographic Institute. http://apdrc.soest.hawaii.edu/datadoc/whoioafluxday.php. Accessed 11 March 2021
Wilkinson JM, Wells H, Field PR, Agnew P (2013) Investigation and prediction of helicopter-triggered lightning over the North Sea. Meteor Appl 20(1):94–106. https://doi.org/10.1002/met.1314
Yavuz V, Özdemir ET, Deniz A (2020) Nowcasting of a thunderstorm: the case study of 2 February, 2015 at Istanbul Ataturk International Airport. Mausam 71(1):21–32
Yavuz V, Özen C, Çapraz Ö, Özdemir ET, Deniz A, Akbayır İ, Temur H (2021a) Analysing of atmospheric conditions and their effects on air quality in Istanbul using Sodar and Ceilometer. Environ Sci Pollut Res. https://doi.org/10.1007/s11356-021-16958-w

Yavuz V, Deniz A, Özdemir ET, Kolay O, Karan H (2021b) Classification and analysis of sea-effect snowbands for Danube Sea area in Black Sea. Int J Climatol 41(5):3139–3152. https://doi.org/10.1002/joc.7010
Yavuz V, Deniz A, Özdemir ET (2021c) Analysis of a vortex causing sea-effect snowfall in the western part of the Black Sea: a case study of events that occurred on 30–31 January 2012. Nat Hazards 108:819–846. https://doi.org/10.1007/s11069-021-04707-8
Yavuz V, Deniz A, Özdemir ET, Karan H, Temiz C (2022a) Long-term thunderstorm analysis at Airports in the Marmara region: types and favourable atmospheric conditions. Int J Global Warming (in press)
Yavuz V, Lupo AR, Fox NI, Deniz A (2022b) Meso-scale comparison of non-sea-effect and sea-effect snowfalls, and development of prediction algorithm for megacity Istanbul Airports in Turkey. Atmosphere 13(5):657. https://doi.org/10.3390/atmos13050657
Yavuz V, Lupo AR, Fox NI, Deniz A (2022c) The role of short-wave troughs on the formation and development of sea-effect snowbands in the western Black Sea. Theor Appl Climatol. https://doi.org/10.1007/s00704-022-04071-y
Ye B, Genio ADD, Lo KKW (1998) CAPE variations in the current climate and in a climate change. J Clim 11(8):1997–2015. https://doi.org/10.1175/1520-0442(1998)011%3c1997:CVITHCC%3e2.0.CO;2
Zhang GJ (2003) Diurnal cycle of convection at the ARM SGP site: role of large-scale forcing, surface fluxes, and convective inhibition. 13th ARM science team meeting proceedings, Broomfield
Zhao W, Duan SB (2020) Reconstruction of daytime land surface temperatures under cloud-covered conditions using integrated MODIS/Terra land products and MSG geostationary satellite data. Remote Sens Environ 247:1–15. https://doi.org/10.1016/j.rse.2020.111931
Zook D (2014) When lightning strikes. Ski Area. Manage 53(4):36